Virus Research 178 (2013) 471–477

Contents lists available at ScienceDirect

Virus Research

journal homepage: www.elsevier.com/locate/virusres

Tick-borne encephalitis virus triggers inositol-requiring enzyme 1 (IRE1) and transcription factor 6 (ATF6) pathways of unfolded protein response☆

Chao Yu[a,*], Katharina Achazi[a,b], Matthias Niedrig[a]

[a] Centre for Biological Threats and Special Pathogens, ZBS 1: Highly Pathogenic Viruses, Robert Koch Institute, Nordufer 20, 13353 Berlin, Germany
[b] Institute of Chemistry and Biochemistry, Freie Universität Berlin, Takustraße 3, 14195 Berlin, Germany

ARTICLE INFO

Article history:
Received 22 May 2013
Received in revised form 15 October 2013
Accepted 21 October 2013
Available online 28 October 2013

Keywords:
Flavivirus
Tick-borne encephalitis virus
ER stress
XBP1
ATF6
Virus replication

ABSTRACT

Tick-borne encephalitis (TBE) is a serious human neurological disease caused by TBE virus (TBEV). However, the mechanisms of TBEV-caused pathogenesis remain unclear. The endoplasmic reticulum (ER) stress response, also defined as the unfolded protein response (UPR), is an important conserved molecular signaling pathway that modulates many biological functions including innate immunity and viral pathogenesis. Here, we investigated the effects of the two UPR signaling pathways upon TBEV infection in Vero E6 cells. We showed that the amount of heat shock protein 72 (Hsp72) increased in the course of TBEV infection. We then confirmed that TBEV infection activates the IRE1 pathway, leading to RNA and protein expression of the spliced X box binding protein 1 (sXBP1). Furthermore, we observed the translocation of ATF6 during TBEV infection and expression of cleaved transcription factor 6 (ATF6) which suggest activation of ATF6 pathway. Finally, we examined whether inhibition of the IRE1 pathway has an effect on TBEV infection. Cell treatment with 3,5-Dibromosalicylaldehyde (IRE1 inhibitor) and tauroursodeoxycholic acid (TUDCA) showed that TBEV replication was significantly limited. These findings provide the first evidence that TBEV infection activates the two UPR signaling pathways. Moreover, inhibition of TBEV replication by UPR inhibitors may provide a novel therapeutic strategy against TBE.

1. Introduction

Tick-borne encephalitis virus, within the genus *Flavivirus* of the family *Flaviviridae*, is an emerging zoonotic virus transmitted by ticks in Europe, the Far East and Asia (Gritsun et al., 2003; Mansfield et al., 2009). It can cause severe infection in humans with a variety of neurological symptoms and diseases (Lindquist and Vapalahti, 2008). In recent years, thousands of diagnosed TBE cases were reported annually, although TBEV infection can be efficiently prevented by vaccination (Demicheli et al., 2009; Donoso Mantke et al., 2011; Suss, 2008). The genome of TBEV consists of a single-stranded positive-sense RNA of about 11 kb in length. It has a single open reading frame which translates for a polyprotein consisting of three structural proteins (C, prM and E) and seven non-structural proteins (NS1, NS2A, NS2B, NS3, NS4A, NS4B and NS5) (Heinz and Allison, 2003). Translation, secretion and modification of the viral proteins as well as virus RNA replication and virus assembly take place at the membranes of the endoplasmic reticulum (ER) and Golgi-derived membranes called vesicle packets (VP). Therefore, TBEV and other flaviviruses modify the ER architecture, resulting in membrane proliferation and hypertrophy of ER, which is beneficial for flavivirus protein secretion and modification (Fernandez-Garcia et al., 2009; Gillespie et al., 2010). Furthermore, reorganized ER protects and maintains newly replicated RNA for the step of virus replication (Miorin et al., 2013).

ER stress is one of the most important cellular reactions caused by virus infection due to high amounts of viral proteins in the ER (He, 2006). The cell reacts to ER stress by activating the unfolded protein response (UPR) pathway which removes misfolded proteins either by attenuating general translation or by enhancing ER folding capacity and ER-associated degradation (Lin et al., 2008). In the ER stress situation, the UPR signaling pathway is mediated by three major transmembrane ER-resident proteins, namely protein kinase RNA-like ER kinase (PERK), activating transcription factor 6 (ATF6) and inositol-requiring enzyme 1 (IRE1) (Ron and Walter, 2007). In the PERK pathway, PERK phosphorylates eukaryotic translation initiation factor 2α (eIF2α), resulting in a decline of protein synthesis (Harding et al., 1999). Activation of the ATF6

* Corresponding author. Tel.: +49 030 18 754 2917; fax: +49 030 18 754 2390.
E-mail address: yuc@rki.de (C. Yu).

0168-1702/$ – see front matter © 2013 The Author. Published by Elsevier B.V. All rights reserved.
http://dx.doi.org/10.1016/j.virusres.2013.10.012

pathway generates an active ATF6 fragment which translocates to the nucleus and up-regulates transcription of UPR genes (Ye et al., 2000). The IRE1 pathway is initiated by IRE1α and controlled by a series of regulators termed as the UPRosome. The UPRosome consists of a complex protein assembled at the ER membrane, such as heat shock protein 72 (Hsp72), apoptosis signal-regulating kinase 1 (ASK1)-interacting protein 1 and the pro-apoptotic proteins Bcl-2-associated X protein (BAX) and Bcl-2 homologous antagonist/killer (BAK) (Hetz, 2012). However, modulation of the IRE1 pathway signaling by these regulators, which associate or dissociate with IRE1α, is cell type dependent. Upon activation of the IRE1 pathway, active IRE1 processes the X box binding protein 1 (XBP1) mRNA by shifting the open reading frame. This results in the expression of the active transcription factor spliced XBP1 (sXBP1), which then up-regulates its target genes (Yoshida et al., 2001).

Recent studies have shown that several flaviviruses preferentially use different UPR pathways to facilitate their replication. Studies with Japanese encephalitis virus (JEV) and Dengue virus (DENV) have shown activation of the IRE1 pathway during infection (Umareddy et al., 2007; Yu et al., 2006). West Nile virus (WNV) modulates all three pathways of the UPR which results in up-regulation of the production of viral RNA and protein (Ambrose and Mackenzie, 2011). Moreover, WNV or JEV infections trigger cell death processes by enhancing the expression of CCAAT/-enhancer-binding protein homologous protein (CHOP) which is a transcription factor induced by the UPR (Medigeshi et al., 2007; Su et al., 2002). Although the effect of these flaviviruses on different UPR pathways has been unveiled, the role of TBEV infection in cellular UPR is still unknown. The goal of our study was to analyze the role of the UPR, in particular regarding the IRE1 pathway and ATF6 pathway in the course of TBEV infection. We first showed that TBEV infection enhanced Hsp72 protein expression which regulates and enhances the IRE1 pathway. We then analyzed that TBEV infection induced the IRE1 pathway, which resulted in high expression of sXBP1. Moreover, we demonstrated that the translocation and expression of the cleaved ATF6, which indicated that ATF6 pathway activation during TBEV infection. Finally, we found that 3,5-Dibromosalicylaldehyde (IRE1 inhibitor) and tauroursodeoxycholic acid (TUDCA), two inhibitors of the UPR, impair TBEV replication. These findings provide new insights into the molecular mechanism of TBEV pathogenesis and may offer a new therapeutic approach to treat TBEV-induced diseases.

2. Materials and methods

2.1. Cell lines and virus strains

Vero E6 cells (ATCC CRL-1586) and A549 cells (ATTC CCL-185) were cultured in 24-well plates and maintained in Dulbecco's modified Eagle's medium (DMEM) supplemented with 10% fetal calf serum, 1% L-glutamine, 1% penicillin and 1% streptomycin. Both cell types were incubated at 37 °C with 5% CO_2. The propagation of the TBEV strain K23 (GenBank accession no. AM600965) was performed in Vero E6 cells (Achazi et al., 2012). Viral titer was determined by plaque assay as described below. Unless stated otherwise, an MOI of 1 was used for the TBEV infection experiments.

2.2. RNA extraction and RT-PCR

The total RNA was extracted from cells using QIAshredder/RNeasy RNA purification columns (Qiagen, Hilden, Germany) following the manufacturer's protocol. cDNA was synthesized from 1 μg of total RNA using Superscript II (Invitrogen, Karlsruhe, Germany) and random hexamer primers (Invitrogen). PCR was performed with the following primer pair: forward primer TTACGAGAGAAAACTCATGGCC and reverse primer GGGTCCAAGTTGTCCAGAATGC (Samali et al., 2010). Glyceraldehyde 3-phosphate dehydrogenase (GAPDH) was used as a loading control with the following primer pair: forward primer CCCATGTTCGTCATGGGTGT and reverse primer: TGGTCATGAGTCCTTCCACGATA (Kurisaki et al., 2003). Cells treated with 1 μg/mL of Tunicamycin (TM) (Sigma–Aldrich, Munich, Germany) for 12 h were used as positive control. TM is an ER stress inducer which inhibits the N-linked protein glycosylation. The products of amplification were separated by electrophoresis on a 3% agarose gel and visualized by ethidium bromide staining. Images were photographed using the Chemidoc system (Bio-Rad, Munich, Germany) and analyzed by the ImageJ 1.42 software.

2.3. ER stress inhibition experiments

To inhibit the ER stress response, the UPR inhibitors IRE1 and TUDCA were used. The IRE1 inhibitor has the salicylaldehyde form of the salicylaldimine and inhibits the IRE1 endoribonuclease activity specifically (Volkmann et al., 2011). TUDCA is a derivative of an endogenous bile acid that alleviates ER stress (Berger and Haller, 2011). Vero E6 cells were pre-treated for 1 h with 60 μM IRE1 inhibitor (Sigma–Aldrich) or 500 μg/mL TUDCA (Calbiochem, Darmstadt, Germany), respectively, and inoculated with TBEV for another hour. Subsequently, cells were washed with PBS to remove the unbound virus particles and were further incubated in the presence of the inhibitors. After 24 and 48 h post infection, respectively, virus-containing cell culture supernatant was analyzed by plaque assay and viral protein from lysed cells was detected by western blotting, respectively, as described below.

2.4. Plaque assay

Virus titers of cell culture supernatants were measured by plaque assay. Briefly, A549 cells were grown overnight in a 24-well plate at 37 °C in 5% CO_2. Serial dilutions of the cell culture supernatant were added to the wells. After an incubation period of 1 h, carboxymethylcellulose (CMC) overlay medium (1.6% CMC in DMEM) was added to each well. The plates were incubated under the same conditions for four days. Each well was fixed by 3.7% formaldehyde for 60 min and stained with Naphthalene Black (1 g of naphthol blue black, 13.6 g of sodium acetate, 60 mL of glacial acetic acid and up to 1 L of ddH_2O). After 1 h, the Naphthalene Black was decanted, the plaques were counted and the calculation of plaque-forming units (PFU) was carried out according to Reed and Muench (1938). Data were shown as PFU/mL.

2.5. Western blotting

Cells were washed twice with ice-cold PBS and lysed using RIPA buffer (50 mM Tris-HCl, pH 8.0, 0.1% SDS, 1% NP40, 150 mM NaCl, 20% glycerol, 2 mM dithiothreitol and 0.5% deoxycholate acid). Nuclear proteins were harvested using the NE-PER nuclear extraction kit (Thermo Scientific). Equivalent amounts of cellular lysates or nuclear proteins were electrophoretically separated by 4–20% Tris-HEPES gels (Thermo Fisher Scientific, Schwerte, Germany). After electrophoresis, proteins were transferred onto a PVDF membrane by using a semi-dry blotter (Thermo Scientific). Then membranes were incubated with blocking buffer (5% non-fat milk in PBS solution with the detergent Tween 20) for 1 h and subsequently incubated with primary antibodies (diluted 1:500 to1:1000) at 4 °C overnight. Anti-TBEV E protein antibody (MAB 1367) was used for detecting TBE virus (Niedrig et al., 1994). Anti-actin and anti-PCNA (Proliferating cell nuclear antigen) antibody was obtained from Cell Signaling Technology (Cell Signaling Technology, Frankfurt am Main, Germany). Anti-XBP1 was obtained

from Santa Cruz Biotechnology (Santa Cruz Biotechnology, Heidelberg, Germany). Anti-ATF6 was purchased from Abcam (Abcam, Bad Nauheim, Germany). After washing three times with PBS solution with Tween 20, membranes were incubated with an appropriate peroxidase-conjugated secondary antibody for 1 h at room temperature (RT). Signal was developed using SuperSignal West Dura Extended Duration Substrate (Thermo Scientific) and detected by the Chemidoc system (Bio-Rad).

2.6. Indirect immunofluorescence microscopy

Vero E6 cells grown on glass coverslips were infected with TBEV strain K23. After 48 h, cells were fixed with 3.7% formaldehyde for 1 h and permeabilized with 0.1% Triton X-100. The coverslips were blocked with blocking buffer (5% bovine serum albumin [BSA] in PBS) for 1 h and incubated with anti-Hsp72 (Enzo life science, Loerrach, Germany) in a 1:200 dilution. After incubation at RT for 1 h, the coverslips were washed three times in PBS and then treated with a goat anti-mouse secondary antibody conjugated to tetramethyl rhodamine isothiocyanate (TRITC) (Dianova, Hamburg, Germany) at a dilution of 1:200. Nuclei were stained with 4′,6-diamidino-2-phenylindole (DAPI). All samples were inspected using a fluorescence microscope (Keyence), and images were analyzed by ImageJ 1.42 software.

2.7. Confocal immunofluorescence microscopy

To generate an ATF6-expressing cell line, Vero E6 cells were transfected with a GFP-ATF6 plasmid using Fugene HD (Roche Diagnostics, Mannheim, Germany), following the manufacturer's instructions. After transfection, cells were incubated with TBEV strain K23 for 24 h. TM (1 μg/mL for 8 h)-treated cells were used as positive controls. Cells were fixed with 3.7% formaldehyde for 1 h and permeabilized with 0.1% Triton X-100 at RT. Samples were incubated with the anti-TBEV E-protein antibody MAB 1367 (1:500) as the first antibody and an Alexa 594-labeled anti-mouse IgG antibody (1:200) (Invitrogen) as the secondary antibody. Coverslips were mounted with ProLong Gold Antifade containing DAPI (Invitrogen), and cells were visualized by LSM780 confocal microscopy (Zeiss, Jena, Germany).

2.8. Apoptosis detection assay

Vero E6 cells grown on glass coverslips overnight were infected with TBEV strain K23. After 48 h, samples were fixed with 3.7% formaldehyde and properly washed with PBS. The apoptotic cells were detected using the TUNEL in situ Cell Death Detection Kit, TMR red (Roche). As positive control, samples were incubated with DNase I (3000 U/mL in 50 mM Tris-HCl, pH 7.5, 1 mg/mL BSA) for 10 min at RT.

2.9. MTT assay

Vero E6 cells were plated into 96-well culture dishes overnight. After removal of the cell culture medium, cells were incubated in the absence (control) or presence of various concentrations of TUDCA or IRE1 inhibitor for 24 and 48 h. Medium was replaced with 20 μL of 3-(4,5-Dimethylthiazol-2-yl)-2,5-diphenyl tetrazolium bromide (MTT) (5 mg/mL) solution and was further incubated at 37 °C. After 4 h, the MTT solution was removed and 200 μL of DMSO were added and gently swirled. After the formazan crystals were dissolved, the optical density was measured at 570 nm using a spectrophotometer (Tecan Group Ltd., Maennedorf, Switzerland).

2.10. Data analysis

Student's *t*-test was performed using Prism 5 software (GraphPad, San Diego, Canada) to compare two sets of data. A *p*-value of less than 0.05 was considered statistically significant.

3. Results

3.1. TBEV infection leads to induction of Hsp72 expression

Hsp72 protein is one of the newly identified components of UPRosome which interacts with IRE1α and regulates IRE1 signaling (Gupta et al., 2010). We first analyzed Hsp72 protein expression over the course of TBEV infection by immunofluorescence. As shown in Fig. 1A, Hsp72 protein expression was persistently increased during the course of infection compared to the control. It is also known that Hsp72 gains its chaperone capacity to deal with different stress situations by migrating to the nucleus (Knowlton et al., 2000). Fig. 1B shows that Hsp72 protein was mostly accumulated in the nucleus 48 h post infection. These results suggest that Hsp72 might induce the IRE1 pathway during TBEV infection.

3.2. TBEV infection activates the IRE1 pathway

In the IRE1 pathway, active IRE1 truncates a 26-nucleotides intron from the unspliced XBP1 (uXBP1) mRNA and generates a cleaved form which encodes a highly active transcription factor, sXBP1 (Yoshida et al., 2001). To detect whether TBEV infection activates the IRE1 pathway, XBP1 mRNA was by RT-PCR using specific primer pairs. As expected, two forms of XBP1 mRNA were detected in the infected cells after virus infection, and a similar result was found in the TM-treated control cells (Fig. 2A). In contrast, sXBP1 could not be detected in untreated and uninfected cells. The induction of sXBP1 apparently increased in TBEV-infected cells at 24 h post infection (Fig. 2B). Furthermore, the protein expression of sXBP1 in the nuclear fractions was at a high level detected by western blotting (Fig. 2C). All together, these results indicate that IRE1 pathway activated during TBEV infection.

3.3. TBEV infection activates the ATF6 pathway

Next, we investigated whether ATF6 was activated in TBEV-infected cells. During ATF6 activation, ATF6 translocates from the ER to the Golgi apparatus where it is processed by site-1 proteases (S1P) and site-2 proteases (S2P). The active fragment of ATF6 then translocates to the nucleus (Haze et al., 1999). Cells transfected with a GFP-ATF6 plasmid and infected with TBEV were used to test this hypothesis by immunofluorescence confocal microscopy. As shown in Fig. 3A (panels a–d), GFP-ATF6 was evenly distributed in the cytoplasmatic ER-like structures and was not translocated to the nucleus in uninfected control cells. However, this characteristic distribution pattern changed after TBEV infection. In Fig. 3A (panels i–l) the TBEV-infected cells show an intense fluorescence near the nucleus, thus indicating that ATF6 is activated by TBEV infection. The same results were found in the TM-treated control cells in Fig. 3A (panels e–h). We then confirmed these observations by monitoring the cleavage of ATF6 expression in the course of TBEV infection. Fig. 3B demonstrated that an induction of ATF6 cleavage detected by western blotting. Taken together, these results show that TBEV infection induces the ATF6 pathway.

3.4. Inhibition of UPR pathway decreases TBEV replication

As the IRE1 pathway is activated by TBEV infection, we wanted to determine whether this pathway was a host antiviral response or facilitated virus replication. Therefore, we tested the effect of the

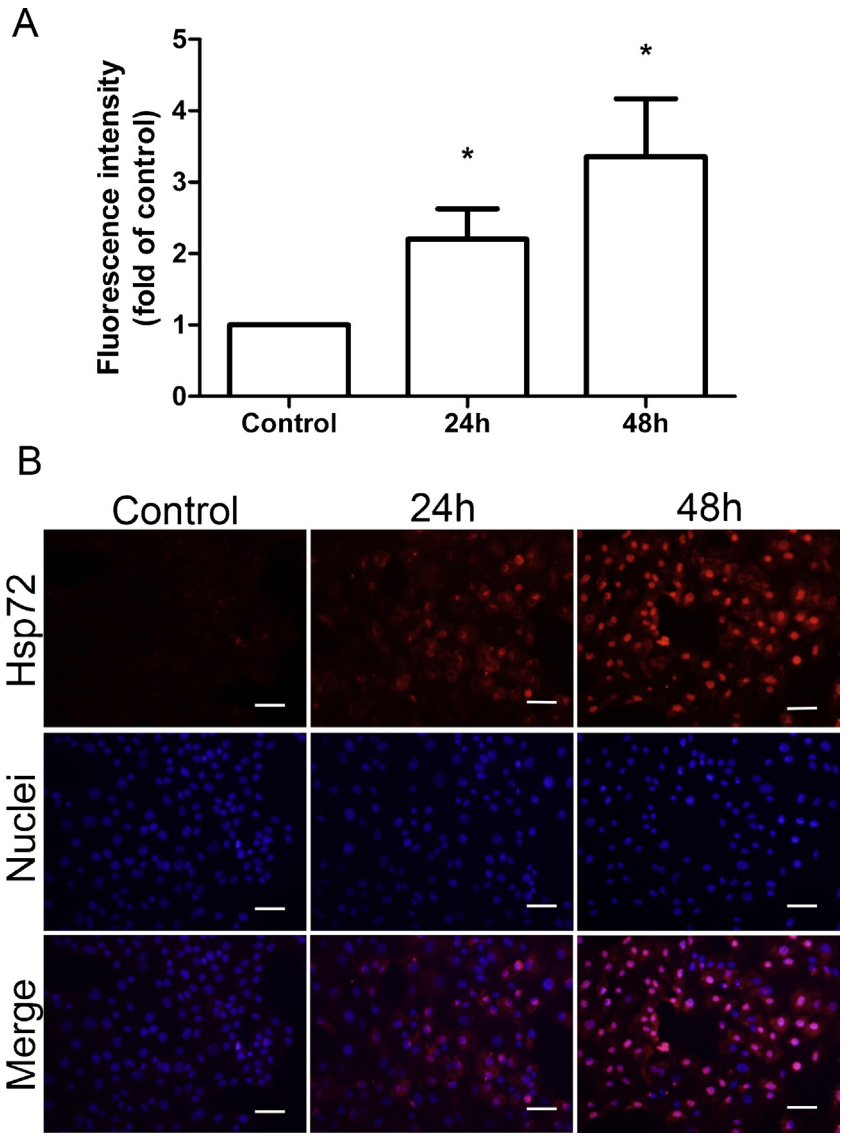

Fig. 1. Increased Hsp72 expression in TBEV-infected cells. (A) TBEV-infected Vero E6 cells were fixed and stained with anti-Hsp72 antibody and DAPI, respectively, at 24 h and 48 h post infection. Uninfected cells cultured for 48 h were used as control. Images show intracellular Hsp72 (red) and cell nuclei (blue) by indirect immunofluorescence staining. Bar chart: 50 μm. (B) The average Hsp72 fluorescence intensity calculated by the ImageJ software in each panel was compared with the control panel. The data were expressed as mean ± SD of three independent experiments. *: $P < 0.05$.

IRE1 inhibitor, a newly identified inhibitor of the IRE1 pathway, on TBEV replication in TBEV-infected cells. In IRE1 inhibitor-pretreated cells the amount of infectious virus particles in the cell culture supernatant was significantly decreased compared to the untreated cells at 24 h post infection (Fig. 4A). Also, western blot analysis revealed that the level of TBEV E-protein expression was reduced in the IRE1 inhibitor-treated cells (Fig. 4C). Interestingly, the amount of infectious virus particles in the cell culture supernatant was slightly increased at 48 h post infection (Fig. 4A) although the level of TBEV-E protein still decreased. This discrepancy suggested that the effect on inhibition of IRE1 pathway only reduced the ER protein folding capacity rather than hampering virus assembly. Meanwhile, TBE virus may utilize the other two UPR pathways to overcome or compensate this inhibition.

Because of these results we wanted to know whether the inhibition of upstream signaling of all three UPR pathways might limit virus replication more efficiently. Therefore, we used the chemical chaperone and UPR inhibitor TUDCA. The inhibition assay was performed as described in the methods section. We observed a sharp decrease of viral protein and infectious virus particles in TUDCA-pretreated cells (Figs. 4B and D). In addition, MTT assay was used to rule out effects by pharmacological inhibition of ER stress on cell viability (Fig. S2). Taken together, the results showed that inhibition of IRE1 pathway, especially inhibition of all three UPR pathways, decreased TBEV replication.

Supplementary material related to this article can be found, in the online version, at http://dx.doi.org/10.1016/j.virusres.2013.10.012.

4. Discussion

Viruses have developed various strategies to exploit cellular host responses for their benefit and survival. In the whole cycle of virus replication, virus activates ER stress by producing viral double-stranded RNA intermediates and huge amounts of viral proteins (He, 2006). Due to their positive-sense genomic RNA, it is important for TBEV to use intracellular membranes to create a suitable microenvironment for replication. After viral particles

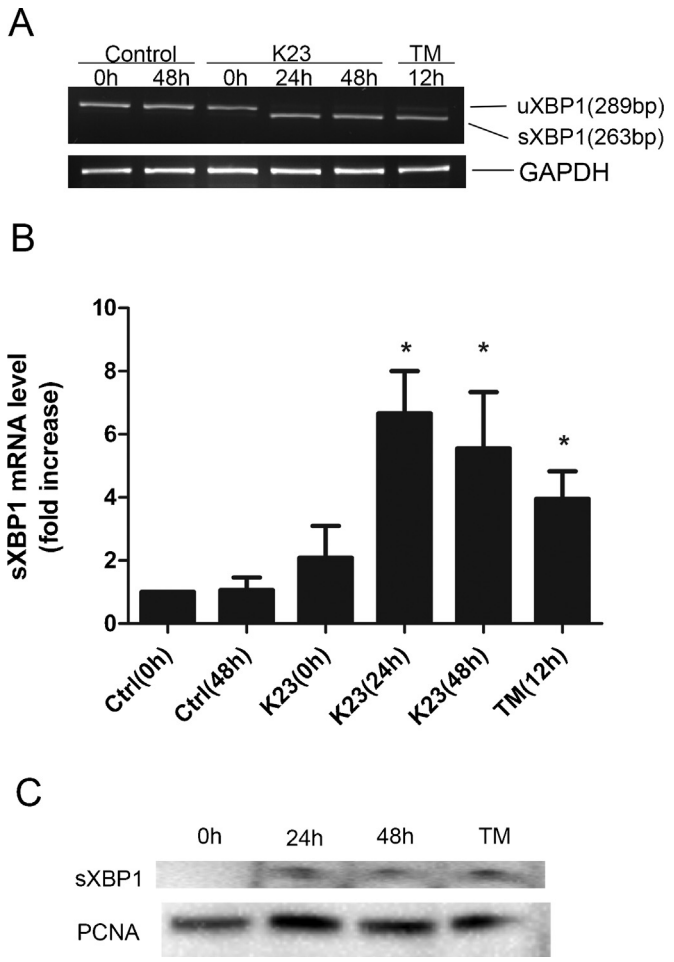

Fig. 2. Induction of spliced XBP1 expression during TBEV infection. (A) XBP1 mRNA was measured by RT-PCR. Vero E6 cells were either infected with TBEV strain K23 or treated with TM (1 μg/mL). XBP1 mRNA was amplified by RT-PCR using XBP1-specific primers. The products were separated by electrophoresis in 3% agarose gels and DNA was visualized by ethidium bromide. The unspliced XBP1 (uXBP1) mRNA was observed as a 289-bp band, and spliced XBP1 (sXBP1) mRNA was observed as a 263-bp band. TM was used as a positive control for the induction of sXBP1. GAPDH mRNA was used as loading control. The representative image was shown. (B) The band intensities of sXBP1 mRNA were measured by ImageJ software and expressed as fold increase compared to control (Ctrl 0 h). *: $P < 0.05$. (C) Western blotting analysis of the spliced XBP1 expression. Nuclear extract were harvested at the indicated times post infection and analyzed by western blotting using an XBP1 antibody. TM treated cells were used as a positive control. The PCNA was used as a nuclear loading control. One of two representative results was shown.

bind to the cell surface, the viral RNA genomes are released into the cytoplasm and used for protein translation (Mandl, 2005). The process of TBEV assembly is detected by electron microscopy in the lumen of the ER and highly associated with cellular ER membrane rearrangements (Overby et al., 2010; Ruzek et al., 2009). Several flaviviruses including WNV, DENV and JEV can activate and regulate the UPR, a cellular stress response to alleviate ER stress caused by the accumulation of viral proteins; however, nothing is known about the regulation of the UPR in TBEV infection (Ambrose and Mackenzie, 2011; Klomporn et al., 2011; Wu et al., 2011).

In this study, we report for the first time that TBEV triggers the IRE1 pathway of the UPR, as the expression of spliced XBP1 mRNA and protein increased in TBEV-infected Vero E6 cells (Fig. 2A and C). Similar results were also observed in the course of JEV and DENV infections (Yu et al., 2006). In contrast, hepatitis C virus replicons inhibit the transactivation of XBP1, demonstrating the various pathogenic mechanisms of different flaviviruses (Tardif et al., 2004). IRE1 pathway activation is downstream of ATF6 activation, and cleavage of ATF6 has been shown to up-regulate the level of XBP1 mRNA (Lee et al., 2002). The cleaved ATF6 moves from the ER to the Golgi complex and translocates to the nucleus. We demonstrated that activated ATF6 was accumulated near the nucleus of TBEV-infected cells (Fig. 3A). We then further confirmed the expression of cleaved ATF6 by western blotting which suggests that TBEV modulate the activation of the ATF6 pathway at the same time (Fig. 3B).

The UPR is initiated to restore normal ER homeostasis during ER stress. Cell death occurs if the balance cannot be sustained (He, 2006). Activation of the IRE1 pathway may enhance the protein-folding ability which alleviates ER stress and reduces cytopathic effects during JEV and DV infection (Yu et al., 2006). In our experiments, we could not find apoptotic cells associated with TBEV infection (Fig. S1). Thus, activation of the IRE1 pathway by TBEV could also be a mechanism to avoid cell death due to virus infection. Moreover, Hsp72, which is known to protect cells from ER stress (Gupta et al., 2010), is highly expressed in TBEV-infected cells (Fig. 1B). We also noticed nuclear accumulation of Hsp72 in TBEV-infected cells (Fig. 1A). This accumulation strengthens the resistance of cells to cellular death (Knowlton et al., 2000). Besides, it was shown for a close relative of TBEV, the hepatitis C virus, that overexpression of Hsp72 enhances viral RNA replication by increasing levels of the replicase complex (Chen et al., 2010). Taken together, we provide evidence that Hsp72 expression and XBP1 activation by TBEV may alleviate UPR which sustains the homeostasis against cell death and facilitates virus replication.

Supplementary material related to this article can be found, in the online version, at http://dx.doi.org/10.1016/j.virusres.2013.10.012.

Because spliced XBP1 is a transcription factor regulating genes responsible for enhancing the protein-folding ability and facilitating the degradation of misfolded protein in the ER, the IRE1 pathway provides an adaptive capacity against ER stress (Lee et al., 2003). We postulated that the IRE1 pathway induced by TBEV supports the cells in handling the ER stress and allows the virus to replicate more efficiently. This would mean inhibition of the UPR would decrease viral replication. Our results show that inhibition of the IRE1 pathway as well as inhibition of all three UPR pathways by IRE1 inhibitor or TUDCA, respectively, caused a reduction in viral titers. As the virus reduction in the TUDCA-treated cells was higher than that in the IRE1 inhibitor-treated cells, more than one UPR-signaling pathway might be involved in TBEV replication. Although the exact mechanisms of host and virus involved in XBP1 splicing and UPR activation have to be further investigated, we show here that TBEV initiated the IRE1 pathway and benefited from the cellular UPR. For this reason, inhibition of the UPR might be a novel option for a therapeutic treatment of TBE.

Recent observations have shown that UPR initiates the inflammation response and regulates cytokine release (Zhang and Kaufman, 2008). TBEV invades the central nervous system by crossing the blood–brain barrier and then causes neural inflammation by its replication (Dumpis et al., 1999). However, TBEV rearranges intracellular membrane compartments and delays the release of inflammation cytokines which facilitate the virus entry into the central nervous system (Overby et al., 2010). UPR-induced inflammation-assisted or -restricted disease progression relies on many factors such as the cell type, disease stage and type of ER sensors (Garg et al., 2012). Further studies in neural cells and mouse models with TBEV infection have to be performed to investigate the role of UPR-mediated inflammation in pathogenesis. Moreover, most TBE cases occur through a tick bite which delivers viruses into the host's circulation system. Dendritic cells are one of the most important cellular components which present antigen and initiate the adaptive immune response during virus invasion (Robertson

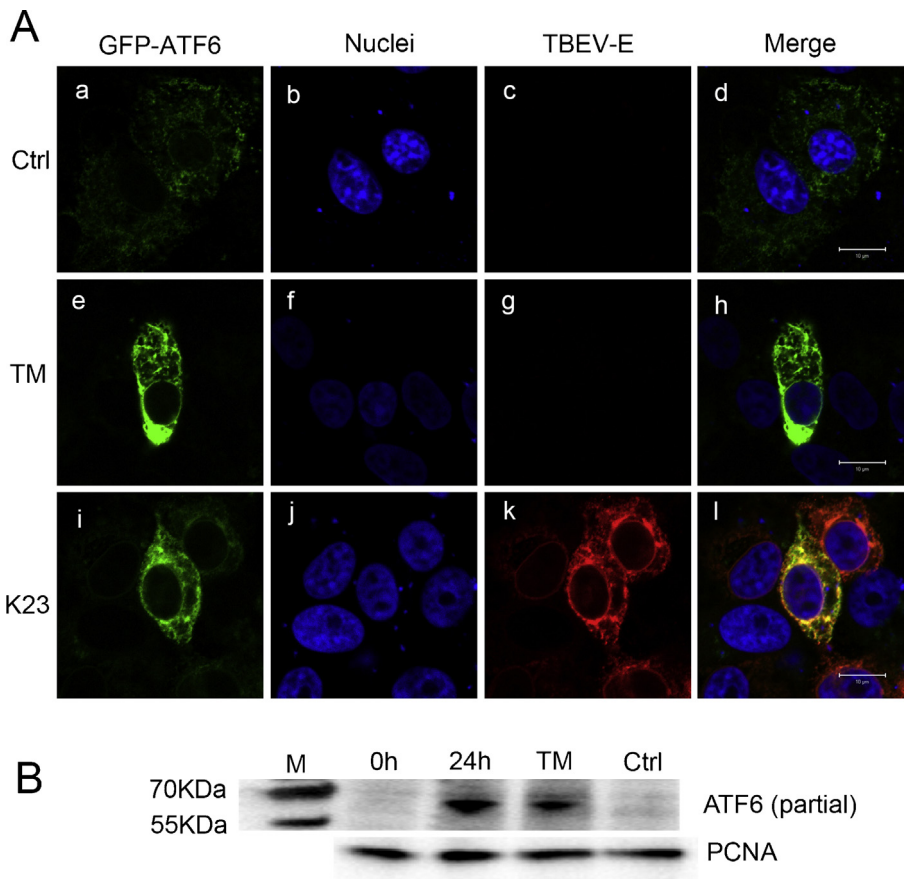

Fig. 3. Analysis of ATF6 pathway during TBEV infection. (A) Relocation of GFP-ATF6 during TBEV infection. GFP-ATF6 plasmids were transiently transfected into Vero E6 cells for 24 h. Then the cells were infected with TBEV strain K23 and further cultured for 24 h (panels i–l) or treated with TM (panels e–h) for 8 h. Untreated and uninfected cells were used as controls (panels a–d). Confocal microscopy was used to detect GFP-ATF6 (green), TBEV E protein (red) and cell nuclei (blue). Bar chart: 10 μm. (B) The expression of ATF6 cleavage from nucleus after TBEV infection was analyzed by western blotting. TM treated cells were used as a positive control for producing ATF6 cleavage. The PCNA was used as a nuclear loading control. One of two representative results was shown.

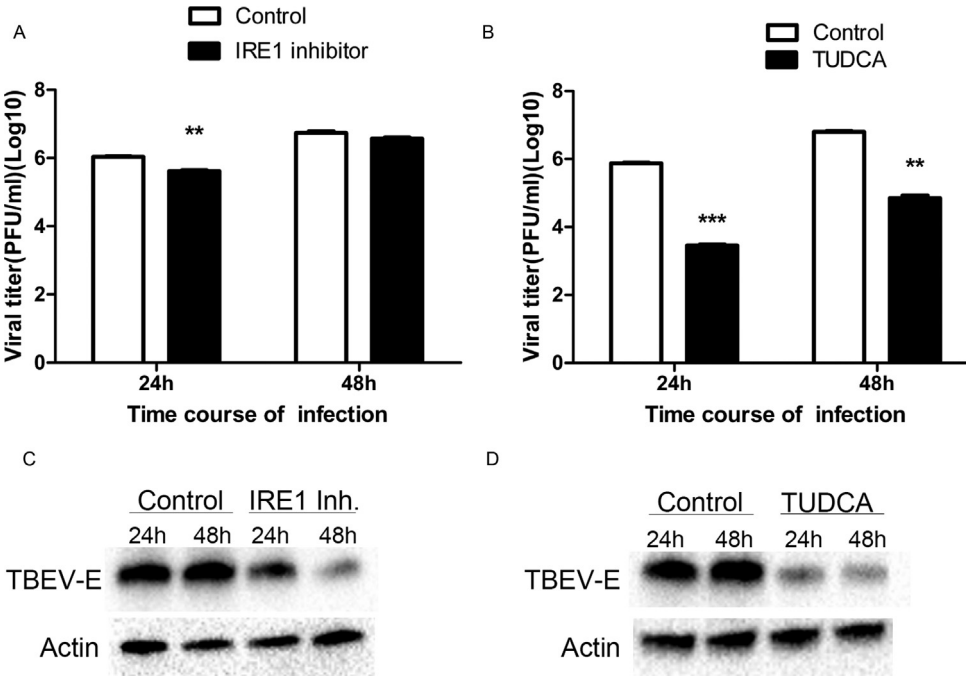

Fig. 4. Effects of UPR inhibitors on the TBEV replication. Vero E6 cells were treated with IRE1 inhibitor (60 μM) or TUDCA (500 μg/mL) for 1 h and then infected with TBEV. (A and B) In the supernatant, virus titers were measured by plaque assay at 24 h and 48 h. The data represent the mean ± SD of three independent experiments. (C and D) Intracellular viral proteins were analyzed by western blot, and representative images were shown at 24 h and 48 h post infection. The virus titers with and without drug treatment at the indicated times were compared with Student's *t* test. **: $P < 0.01$; ***: $P < 0.001$.

et al., 2009). However, MHC class I molecules displayed on the cell surface of dendritic cells are impaired by the ER stress response (Granados et al., 2009; Ulianich et al., 2011). This phenomenon caused by ER stress response may be harmful for the dendritic cells presenting viral antigens and inhibit the host's antiviral response.

In conclusion, our report provides the first evidence that TBEV infection activates the IRE1 pathway and ATF6 pathway of the UPR and strongly up-regulates the expression of Hsp72. Furthermore, pharmacological treatment of the UPR pathway has decreased TBEV replication which might suggest a new route of antiviral therapy.

Acknowledgements

GFP-ATF6 plasmid was kindly provided by Professor R. Prywes (Columbia University, New York). We thank Dr. Kazimierz Madela and Dr. Christoph Curths for technical support in the confocal microscopy work. We also acknowledge Dr. Litzba Nadine and Ursula Erikli for copy-editing. Chao Yu is supported by the China Scholarship Council (CSC 2009617027).

References

Achazi, K., Patel, P., Paliwal, R., Radonic, A., Niedrig, M., Donoso-Mantke, O., 2012. RNA interference inhibits replication of tick-borne encephalitis virus in vitro. Antiviral Research 93 (1), 94–100.

Ambrose, R.L., Mackenzie, J.M., 2011. West Nile virus differentially modulates the unfolded protein response to facilitate replication and immune evasion. Journal of Virology 85 (6), 2723–2732.

Berger, E., Haller, D., 2011. Structure-function analysis of the tertiary bile acid TUDCA for the resolution of endoplasmic reticulum stress in intestinal epithelial cells. Biochemical and Biophysical Research Communications 409 (4), 610–615.

Chen, Y.J., Chen, Y.H., Chow, L.P., Tsai, Y.H., Chen, P.H., Huang, C.Y., Chen, W.T., Hwang, L.H., 2010. Heat shock protein 72 is associated with the hepatitis C virus replicase complex and enhances viral RNA replication. Journal of Biological Chemistry 285 (36), 28183–28190.

Demicheli, V., Debalini, M.G., Rivetti, A., 2009. Vaccines for preventing tick-borne encephalitis. Cochrane Database of Systematic Reviews 1, CD000977.

Donoso Mantke, O., Escadafal, C., Niedrig, M., Pfeffer, M., Working Group For Tick-Borne Encephalitis Virus C, 2011. Tick-borne encephalitis in Europe, 2007 to 2009. Euro Surveillance: Bulletin Europeen sur les maladies transmissibles = European Communicable Disease Bulletin 16 (39).

Dumpis, U., Crook, D., Oksi, J., 1999. Tick-borne encephalitis. Clinical Infectious Diseases: An Official Publication of the Infectious Diseases Society of America 28 (4), 882–890.

Fernandez-Garcia, M.D., Mazzon, M., Jacobs, M., Amara, A., 2009. Pathogenesis of flavivirus infections: using and abusing the host cell. Cell Host & Microbe 5 (4), 318–328.

Garg, A.D., Kaczmarek, A., Krysko, O., Vandenabeele, P., Krysko, D.V., Agostinis, P., 2012. ER stress-induced inflammation: does it aid or impede disease progression? Trends in Molecular Medicine 18 (10), 589–598.

Gillespie, L.K., Hoenen, A., Morgan, G., Mackenzie, J.M., 2010. The endoplasmic reticulum provides the membrane platform for biogenesis of the flavivirus replication complex. Journal of Virology 84 (20), 10438–10447.

Granados, D.P., Tanguay, P.L., Hardy, M.P., Caron, E., de Verteuil, D., Meloche, S., Perreault, C., 2009. ER stress affects processing of MHC class I-associated peptides. BMC Immunology 10, 10.

Gritsun, T.S., Lashkevich, V.A., Gould, E.A., 2003. Tick-borne encephalitis. Antiviral Research 57 (1–2), 129–146.

Gupta, S., Deepti, A., Deegan, S., Lisbona, F., Hetz, C., Samali, A., 2010. HSP72 protects cells from ER stress-induced apoptosis via enhancement of IRE1alpha-XBP1 signaling through a physical interaction. PLoS Biology 8 (7), e1000410.

Harding, H.P., Zhang, Y., Ron, D., 1999. Protein translation and folding are coupled by an endoplasmic-reticulum-resident kinase. Nature 397 (6716), 271–274.

Haze, K., Yoshida, H., Yanagi, H., Yura, T., Mori, K., 1999. Mammalian transcription factor ATF6 is synthesized as a transmembrane protein and activated by proteolysis in response to endoplasmic reticulum stress. Molecular Biology of the Cell 10 (11), 3787–3799.

He, B., 2006. Viruses, endoplasmic reticulum stress, and interferon responses. Cell Death and Differentiation 13 (3), 393–403.

Heinz, F.X., Allison, S.L., 2003. Flavivirus structure and membrane fusion. Advances in Virus Research 59, 63–97.

Hetz, C., 2012. The unfolded protein response: controlling cell fate decisions under ER stress and beyond. Nature Reviews Molecular Cell Biology 13 (2), 89–102.

Klomporn, P., Panyasrivanit, M., Wikan, N., Smith, D.R., 2011. Dengue infection of monocytic cells activates ER stress pathways, but apoptosis is induced through both extrinsic and intrinsic pathways. Virology 409 (2), 189–197.

Knowlton, A.A., Grenier, M., Kirchhoff, S.R., Salfity, M., 2000. Phosphorylation at tyrosine-524 influences nuclear accumulation of HSP72 with heat stress. American Journal of Physiology: Heart and Circulatory Physiology 278 (6), H2143–H2149.

Kurisaki, K., Kurisaki, A., Valcourt, U., Terentiev, A.A., Pardali, K., Ten Dijke, P., Heldin, C.H., Ericsson, J., Moustakas, A., 2003. Nuclear factor YY1 inhibits transforming growth factor beta- and bone morphogenetic protein-induced cell differentiation. Molecular and Cellular Biology 23 (13), 4494–4510.

Lee, K., Tirasophon, W., Shen, X., Michalak, M., Prywes, R., Okada, T., Yoshida, H., Mori, K., Kaufman, R.J., 2002. IRE1-mediated unconventional mRNA splicing and S2P-mediated ATF6 cleavage merge to regulate XBP1 in signaling the unfolded protein response. Genes & Development 16 (4), 452–466.

Lee, A.H., Iwakoshi, N.N., Glimcher, L.H., 2003. XBP-1 regulates a subset of endoplasmic reticulum resident chaperone genes in the unfolded protein response. Molecular and Cellular Biology 23 (21), 7448–7459.

Lin, J.H., Walter, P., Yen, T.S., 2008. Endoplasmic reticulum stress in disease pathogenesis. Annual Review of Pathology 3, 399–425.

Lindquist, L., Vapalahti, O., 2008. Tick-borne encephalitis. Lancet 371 (9627), 1861–1871.

Mandl, C.W., 2005. Steps of the tick-borne encephalitis virus replication cycle that affect neuropathogenesis. Virus Research 111 (2), 161–174.

Mansfield, K.L., Johnson, N., Phipps, L.P., Stephenson, J.R., Fooks, A.R., Solomon, T., 2009. Tick-borne encephalitis virus – a review of an emerging zoonosis. Journal of General Virology 90 (Pt 8), 1781–1794.

Medigeshi, G.R., Lancaster, A.M., Hirsch, A.J., Briese, T., Lipkin, W.I., Defilippis, V., Fruh, K., Mason, P.W., Nikolich-Zugich, J., Nelson, J.A., 2007. West Nile virus infection activates the unfolded protein response, leading to CHOP induction and apoptosis. Journal of Virology 81 (20), 10849–10860.

Miorin, L., Romero-Brey, I., Maiuri, P., Hoppe, S., Krijnse-Locker, J., Bartenschlager, R., Marcello, A., 2013. Three dimensional architecture of tick-borne encephalitis virus replication sites and trafficking of the replicated RNA. Journal of Virology 87 (11), 6469–6481.

Niedrig, M., Klockmann, U., Lang, W., Roeder, J., Burk, S., Modrow, S., Pauli, G., 1994. Monoclonal antibodies directed against tick-borne encephalitis virus with neutralizing activity in vivo. Acta Virologica 38 (3), 141–149.

Overby, A.K., Popov, V.L., Niedrig, M., Weber, F., 2010. Tick-borne encephalitis virus delays interferon induction and hides its double-stranded RNA in intracellular membrane vesicles. Journal of Virology 84 (17), 8470–8483.

Reed, L.J., Muench, H., 1938. A simple method of estimating fifty percent endpoints. The American Journal of Hygiene 27, 493–497.

Robertson, S.J., Mitzel, D.N., Taylor, R.T., Best, S.M., Bloom, M.E., 2009. Tick-borne flaviviruses: dissecting host immune responses and virus countermeasures. Immunologic Research 43 (1–3), 172–186.

Ron, D., Walter, P., 2007. Signal integration in the endoplasmic reticulum unfolded protein response. Nature Reviews Molecular Cell Biology 8 (7), 519–529.

Ruzek, D., Vancova, M., Tesarova, M., Ahantarig, A., Kopecky, J., Grubhoffer, L., 2009. Morphological changes in human neural cells following tick-borne encephalitis virus infection. Journal of General Virology 90 (Pt 7), 1649–1658.

Samali, A., Fitzgerald, U., Deegan, S., Gupta, S., 2010. Methods for monitoring endoplasmic reticulum stress and the unfolded protein response. International Journal of Cell Biology 2010, 830307.

Su, H.L., Liao, C.L., Lin, Y.L., 2002. Japanese encephalitis virus infection initiates endoplasmic reticulum stress and an unfolded protein response. Journal of Virology 76 (9), 4162–4171.

Suss, J., 2008. Tick-borne encephalitis in Europe and beyond–the epidemiological situation as of 2007. Euro Surveillance: Bulletin Europeen sur les maladies transmissibles = European Communicable Disease Bulletin 13 (26).

Tardif, K.D., Mori, K., Kaufman, R.J., Siddiqui, A., 2004. Hepatitis C virus suppresses the IRE1-XBP1 pathway of the unfolded protein response. Journal of Biological Chemistry 279 (17), 17158–17164.

Ulianich, L., Terrazzano, G., Annunziatella, M., Ruggiero, G., Beguinot, F., Di Jeso, B., 2011. ER stress impairs MHC Class I surface expression and increases susceptibility of thyroid cells to NK-mediated cytotoxicity. Biochimica et Biophysica Acta 1812 (4), 431–438.

Umareddy, I., Pluquet, O., Wang, Q.Y., Vasudevan, S.G., Chevet, E., Gu, F., 2007. Dengue virus serotype infection specifies the activation of the unfolded protein response. Virology Journal 4, 91.

Volkmann, K., Lucas, J.L., Vuga, D., Wang, X., Brumm, D., Stiles, C., Kriebel, D., Der-Sarkissian, A., Krishnan, K., Schweitzer, C., Liu, Z., Malyankar, U.M., Chiovitti, D., Canny, M., Durocher, D., Sicheri, F., Patterson, J.B., 2011. Potent and selective inhibitors of the inositol-requiring enzyme 1 endoribonuclease. Journal of Biological Chemistry 286 (14), 12743–12755.

Wu, Y.P., Chang, C.M., Hung, C.Y., Tsai, M.C., Schuyler, S.C., Wang, R.Y., 2011. Japanese encephalitis virus co-opts the ER-stress response protein GRP78 for viral infectivity. Virology Journal 8, 128.

Ye, J., Rawson, R.B., Komuro, R., Chen, X., Dave, U.P., Prywes, R., Brown, M.S., Goldstein, J.L., 2000. ER stress induces cleavage of membrane-bound ATF6 by the same proteases that process SREBPs. Molecular Cell 6 (6), 1355–1364.

Yoshida, H., Matsui, T., Yamamoto, A., Okada, T., Mori, K., 2001. XBP1 mRNA is induced by ATF6 and spliced by IRE1 in response to ER stress to produce a highly active transcription factor. Cell 107 (7), 881–891.

Yu, C.Y., Hsu, Y.W., Liao, C.L., Lin, Y.L., 2006. Flavivirus infection activates the XBP1 pathway of the unfolded protein response to cope with endoplasmic reticulum stress. Journal of Virology 80 (23), 11868–11880.

Zhang, K., Kaufman, R.J., 2008. From endoplasmic-reticulum stress to the inflammatory response. Nature 454 (7203), 455–462.